ISSN 0918-6638

NIFS--373

JP9601146

Control of Discharge Conditions to Reduce Hydrogen Content in Low Z Films Produced with DC Glow

M. Natsir, A. Sagara, K. Tsuzuki, B. Tsuchiya,
Y. Hasegawa, O. Motojima

(Received - Aug. 23, 1995)

NIFS-373 Sep. 1995

Control of Discharge Conditions to Reduce Hydrogen Content in Low Z films Produced with DC Glow

M. Natsir, A. Sagara*, K. Tsuzuki,

B. Tsuchiya**, Y. Hasegawa***, O. Motojima*

The Graduate University for Advanced Studies,
Department of Nuclear Fusion Science, Furo-cho Chikusa-ku Nagoya 464-01, Japan
* National Institute for Fusion Science, Furo-cho Chikusa-ku Nagoya 464-01, Japan
** Nagoya University, Department of Crystalline Materials Science,
Furo-cho Chikusa-ku Nagoya 464-01, Japan
*** Nagoya University, Department of Energy Engineering and Science,
Furo-cho Chikusa-ku Nagoya 464-01, Japan

ABSTRACT

Boronization at near room temperature has been performed in plasma processing teststand (PPT) by using a 5 % diborane gases B_2H_6 in He on electrically floating or unfloating Al samples under various conditions on DC glow discharge power or total gas pressure. The hydrogen concentration was analyzed by using elastic recoil detection method (ERD) and a new modified normalizing technique with Rutherford back scattering (RBS). Results showed that a high growth rate of film formation and floating surface were effective in reducing hydrogen concentration in B films. This result was in good agreement with earlier measurements of H with flash filament (FF) desorption method. In particular the H/B ratio was reduced by decreasing ions but increasing radicals for B film formation.

Key words: DC glow, boronization, elastic recoil detection, hydrogen content, H recycling, LHD.

1. INTRODUCTION

Control of hydrogen particle recycling on plasma facing materials is considered to be one of key issues to improve plasma performance in Large Helical Device [1,2]. In LHD, on the other hand, low Z coating such as boronization of wall surfaces is considered as the main technique of wall conditioning, because the vacuum vessel is allowed to be baked at only the temperature below 100 ^{o}C [3,4]. In this low temperature range, however, hydrogen atoms contained in low Z films formed with such as boronization or carbonization are known to be thermally desorbed not so sufficiently [5] as performed in TEXTOR [6], DIII-D [7], and JT-60U [8] at elevated wall temperature above 200 ^{o}C, resulting in good control of hydrogen recycling and significant improvement of the plasma parameters.

So far, in our experiments, the hydrogen content in boronized or carbonized films produced at room temperature was successfully reduced by controlling glow discharge conditions. The low Z coated film was produced using the gas mixtures of decaborane $B_{10}H_{14}$ and He or pure CH_4 in DC glow discharge. The results showed that the hydrogen content decreased with the increase of the growth rate of film formation [9-10].

In our previous works the H content were measured by flash filament (FF) desorption method or residual gas analysis (RGA). FF was set at electrically floating potential to avoid heating up due to discharge current. In this work to make clear the difference between floating and unfloating, B coated films were prepared on floating or unfloating samples, and depth profiles of H were analyzed with ERD technique. For this purpose, new modified method using RBS was established to monitor the probing ion flux. The results using ERD were compared with conventional method of FF or RGA.

2. EXPERIMENTAL

2.1. Discharge conditions and film depositions

Experiments on controlling the hydrogen content were systematically performed by using Plasma Processing Teststand (PPT) facility. A schematic diagram of the experimental set-up is shown in Fig.1. The principle of the controlling discharge conditions and the experimental set-up have been described in elsewhere [9-10]. For the present work, two pure aluminum sample plates (99.999%) with the size of 20x10x1mm were set on the sample holder and placed on the cathode (liner) so that the sample surfaces to be exposed to a plasma were under the same geometrical condition. The surface temperatures of floating, unfloating, the liner, the quartz oscillator, the flash filament and anode were monitored with a thermocouple and an infrared TV camera in order to maintain liner and substrate surface temperature T below 150 ^{o}C, under which thermal desorption of H from B film is negligible [5]. Here, it is noted that, except for the quartz oscillator, all discharge systems were isolated from the ground to make the discharge at only the inside of the cathode.

After evacuated below 10^{-6} Torr, sample gases B_2H_6 and He were introduced into the chamber with typical flow rates in the range of 5 to 50 sccm and the pressure in the range of 60 to 200 mTorr by adjusting pumping speed. Coated films were prepared under DC glow discharge with the input power of 80 to 300 W at the voltage between 300 to 600 V or 0.2 A to 0.5 A. During the discharge the operation parameters were fixed at almost constant conditions, and the plasma was analyzed using a Langmuir probe before fully contaminated the probe surface under coating.

By considering the maximum sampling depth and depth resolution of ERD, the optimum thickness of boron film was estimated to be about 100 nm. During film formation for 5 ~ 15 min, however, the surface temperature of samples increased and discharge were stopped at temperature near 150 ^{o}C and cooled down. This procedure was repeated for 0 to few times to produce the 100 nm thick film depending on discharge conditions.

After each boronization, the system pumping speed was readjusted to 4 l/s with He, then the FF was flashed with monitoring desorbed H_2 with RGA. Lastly, the coated samples were taken out to atmosphere from the chamber for H content and thickness measurements with ion beam analysis as described below.

2. 2. Determination of hydrogen during film growth.

In order to measure hydrogen content and depth profiling the ion beam analysis of ERD by using 1.5 MeV He^{+} ions was performed. Experimental set-up was the same with that described in [2,11]. The ion beam for depth profiling was 1.5 MeV He^{+} impinging on the target making an the incident angle of the ion beam was set at 10 ^{o} from the sample surface. A solid state detector of ERD for recoiled H atoms was placed at the forward scattering angle of 20 ^{o} from the probe beam, with a mylar filter of 6 μm thick at the front of the detector to cut the scattered He ions from the target [11]. In order to measure the probing ion fluence, the RBS detector was set at 150 ^{o} from the probe beam as shown in Fig.2.

3. RESULTS and DISCUSSION

Figure 2 shows a typical RBS spectrum taken from the unfloating B coated Al sample, on which B can't be clearly observed, probably due to

surface roughness of Al target. The B film thickness was measured from the shift of the Al surface edge as shown in Fig. 2. Then Al edge intensity with calculated scattering cross section σ and energy stopping power ε under the B film was used as the measure of the probing He^+ fluences which was used to obtain absolute H concentration from ERD spectra. This method was newly established in this work for the use in the case of low Z thin films.

Figure 3 shows the hydrogen atom profiles in boron films formed on floating or unfloating Al samples. The ERD data processing program was calibrated by using a vanadium hydride (V_2H) standard sample. The atomic density ρ_B of the B film was supposed to be 1.5 g/cm^3 [6]. From this figure it is observed that the H profile on the unfloated sample is more dense, flat, and thick in comparison with the floated one. These results will be discussed later.

Figures 4(a) and (b) shows the peak H/B atomic ratio and the film growth rate measured by ERD and RBS as a function of the discharge power and total gas pressure, respectively. From both figures it can be observed that the H/B are reduced with increasing the film growth rate when the discharge power is increased, or when the total pressure is increased. These results are in good agreement with our results obatained so far from the FF method or RGA [9-10].

The film growth rate gives the B atoms flux ϕ_{BU} and ϕ_{BF} for unfloating and floating cases, respectively. Here it may be supposed that ϕ_{BU} consists of B_nH_m ions and neutrals, that is, radicals, and ϕ_{BF} consists of mainly radicals, because, under glow discharge, ions are mainly produced in the cathode sheath due to electron impact and they are mostly extracted to the cathode surface which has deeper negative potential of about 500 V on the unfloating sample than that of a several V on the floating sample. Therefore $\phi_{BU} - \phi_{BF}$ may gives B atom flux in forms of $B_nH_m^+$. From Fig. 5 (a) and (b) it is clearly observed that the H/B ratio is reduced with reducing the ionic flux ($\phi_{BU} - \phi_{BF}$). It is also

observed that, though the ionic flux contributes to increasing the film growth rate as shown in Fig. 4, it is better to increase the radical flux ϕ_{BF} to reduce the H/B ratio.

To explain the difference between ions and radicals regarding growth of B film and reduction of H/B ratio, there must be considered two aspects, that is, the difference of molecular forms concerning B and H, and the difference of surface reactions such as impact desorption, recoil implantation and/or surface recombination of H atoms depending on kinetic energies of impinging particles including He^+ ions. Within this work it is not easy to evaluate these aspects quantitatively, and more detailed experiments will be needed, comparing with complementary modeling calculations.

4. CONCLUSION

Boronization at near room temperature was performed from diborane gases B_2H_6 on electrically floating or unfloating Al samples under various conditions on DC glow discharge power or total gas pressure. The hydrogen concentration was analyzed by using elastic recoil detection method (ERD) and a new modified normalizing technique with Rutherford back scattering (RBS) was introduced. Results showed that a high growth rate of film formation and floating surface were effective in reducing hydrogen concentration in B films. This result was in good agreement with earlier measurements of H with flash filament (FF) desorption method. In particular, due to advantage of using floating and unfloating samples, contributions of ionic and radical fluxes were separately characterized, resulting that the H/B ratio is reduced by decreasing the ionic flux but increasing the radical one for B film formation.

Acknowledgments

We acknowledge the sharing of machine time of the Van de Graaff accelerator with Prof. K. Morita and his staff of Nuclear Engineering Department of Nagoya University.

REFERENCES

[1] N. Ohyabu, et. al, J. Nucl. Mater., **220-222** (1995) 298-301.

[2] A. Sagara, et. al, J. Nucl. Mater., **220-222** (1995) 627-630.

[3] A. Sagara, et. al, NIFS Annual Report., (1992) 11.

[4] N. Noda, et. al, J. Nucl. Mater., **220-222** (1995) 623-626.

[5] H. Toyoda, et. al, Appl. Phys. Lett., **51** (1987) 11.

[6] J. Winter, et. al, J. Nucl. Mater., **176&177** (1990)13-31.

[7] G.L. Jackson, et. al, J. Nucl. Mater., **196&198** (1992) 236-240.

[8] M. Saidoh, et. al, Jpn. J. Appl. Phys., **32**, 7, (1993) 3276-3281.

[9] M. Natsir, A. Sagara, et. al, J. Nucl. Mater., **220-222** (1995) 865-868.

[10] M. Natsir, et. al, Trans. of Fusion. Tech., **27** (1995) 527-531.

[11] K. Kamada, A. Sagara, et. al, J. Nucl. Mater., **128-129** (1984) 664.

FIGURE CAPTIONS :

Fig. 1. The schematic illustration of the PPT device with showing locations of the samples.

Fig. 2. RBS spectra taken from B films prepared on electrically unfloating Al samples.

Fig. 3. Depth profiles of hydrogen atom in boron films on electrically floating or unfloating Al samples.

Fig. 4(a). Discharge power dependence of H/B peak ratio in depth profile and growth rate on the floating or unfloating Al samples.

Fig. 4(b). Total gas pressure dependence of H/B peak ratio in depth profile and growth rate on the floating or unfloating Al samples.

Fig. 5(a). Relation between the H/B ratio and the B molecules flux on the floating or unfloating Al samples under the discharge power dependence.

Fig. 5(b). Relation between the H/B ratio and the B molecules flux on the floating or unfloating Al samples under the total discharge pressure dependence.

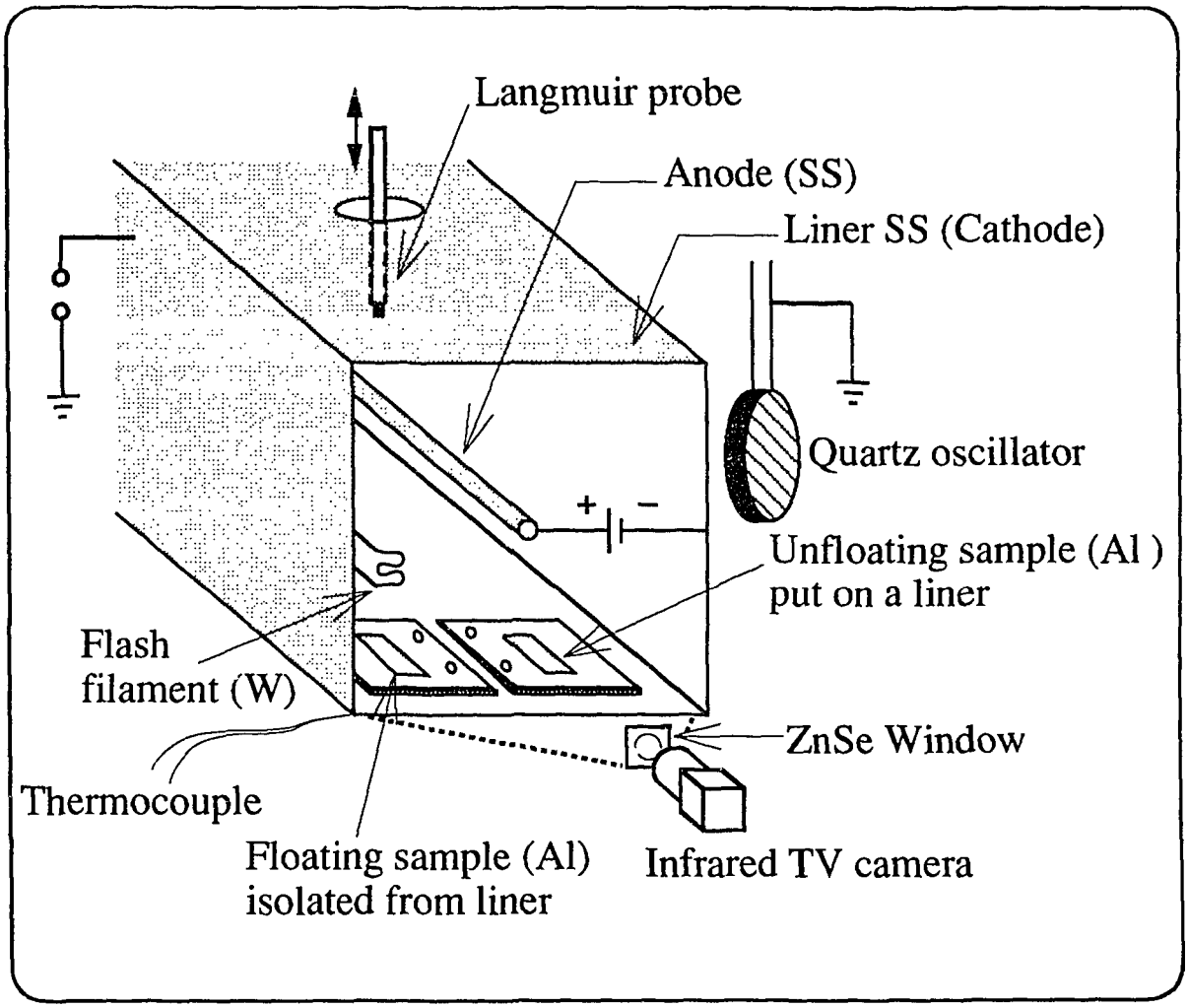

Figure 1, M. Natsir, et. al.

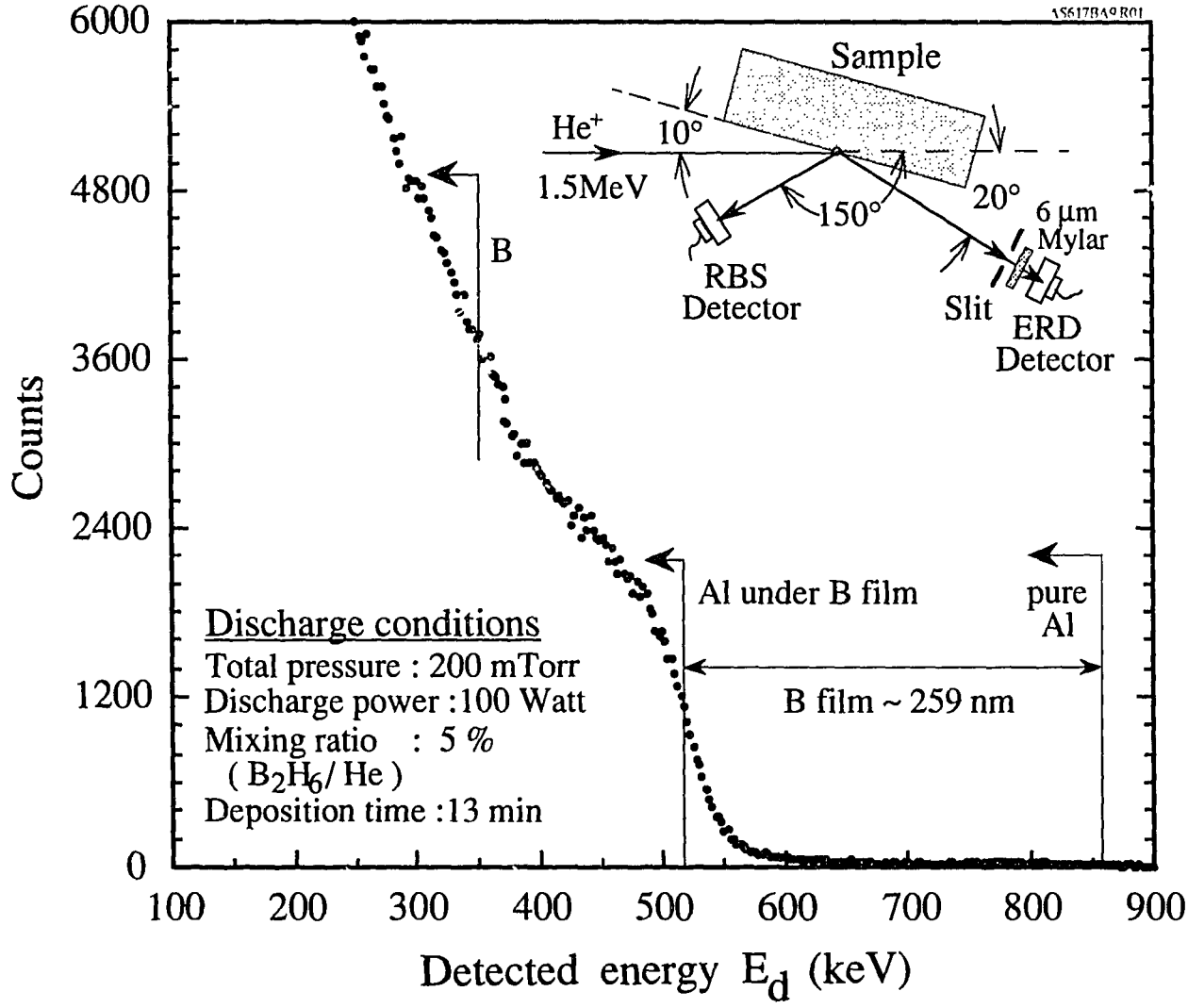

Figure 2, M. Natsir, et. al.

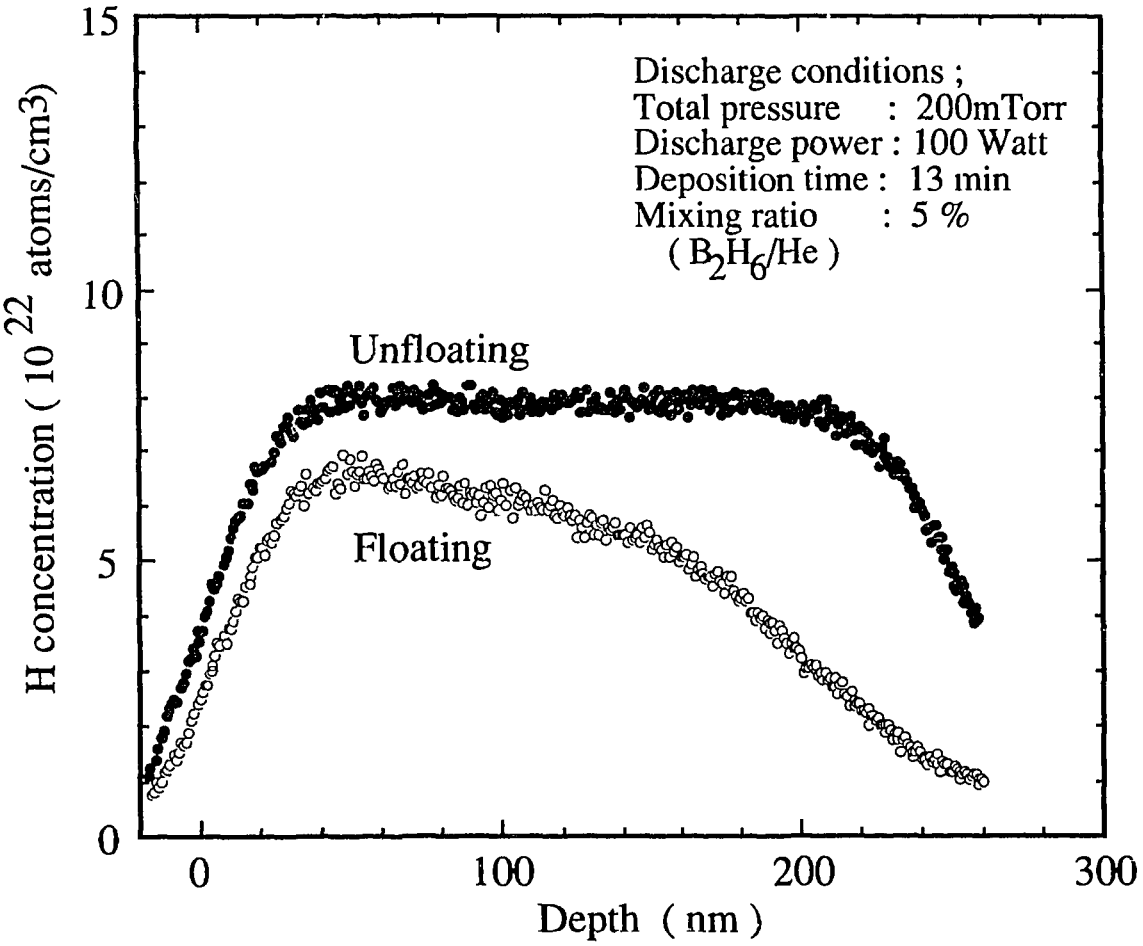

Fig. 3. M. Natsir, et. al.

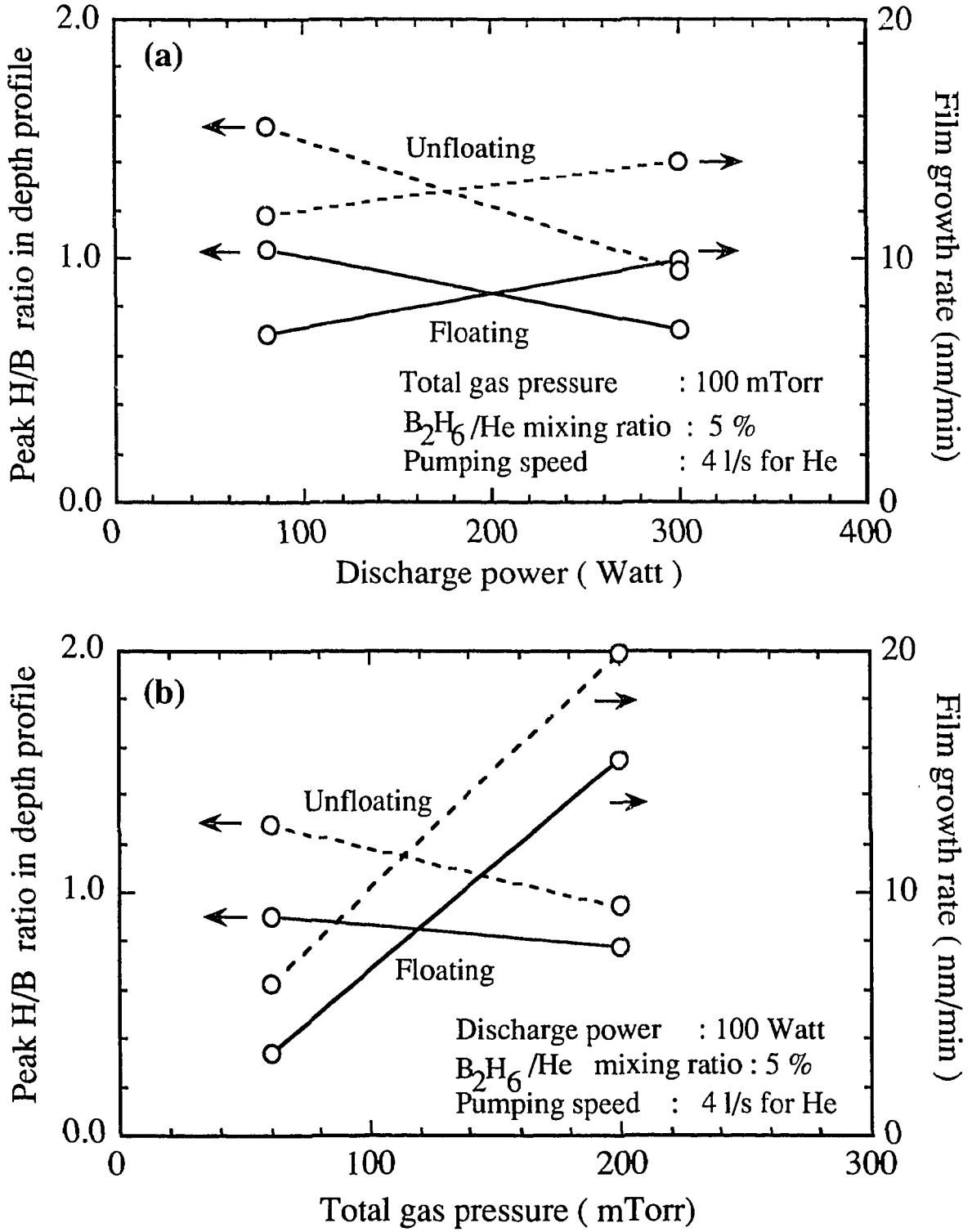

Figure 4, M. Natsir, et. al.

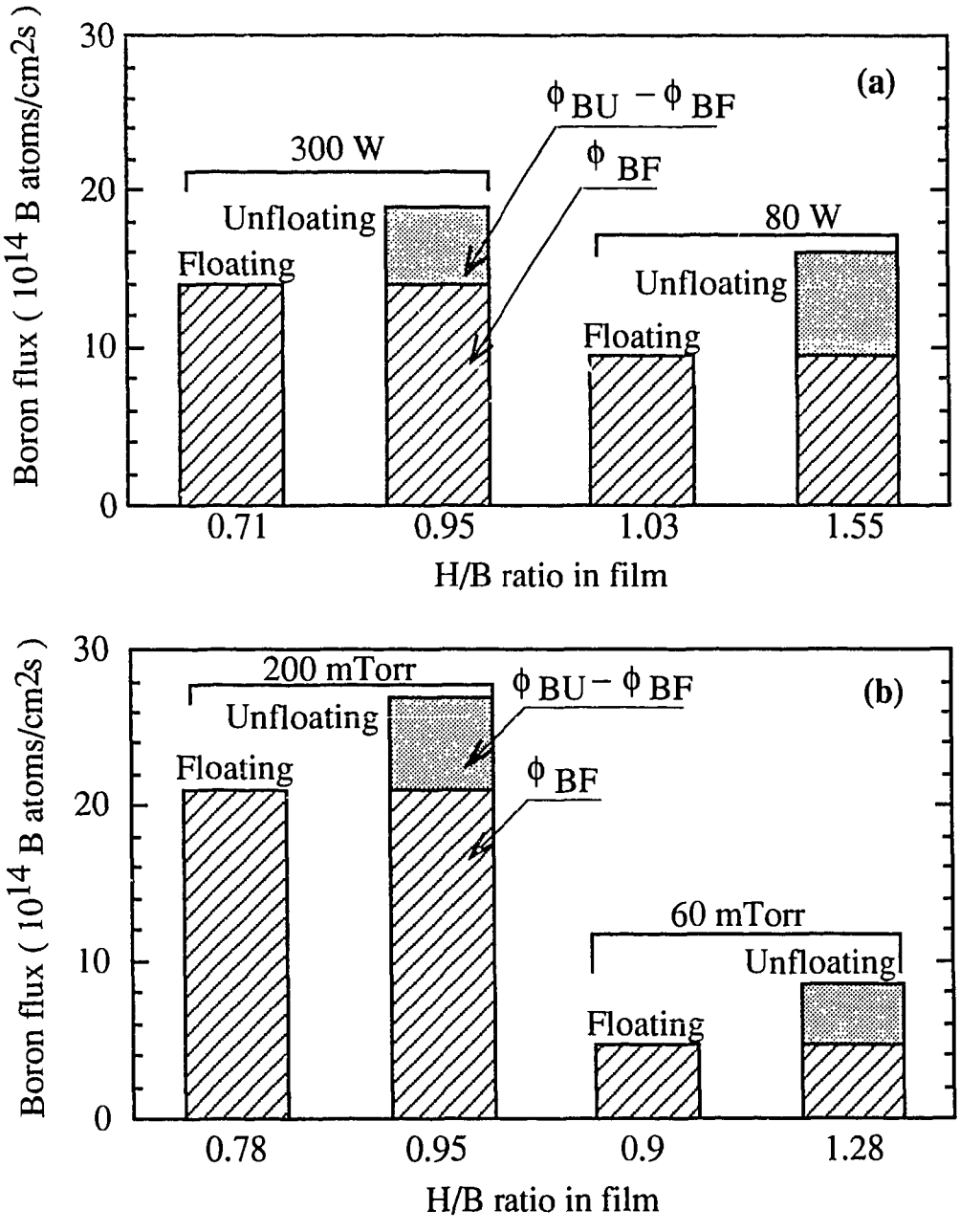

Figure 5, M. Natsir, et. al.

Recent Issues of NIFS Series

NIFS-325 A. Taniike, M. Sasao, Y. Hamada, J. Fujita, M. Wada,
The Energy Broadening Resulting from Electron Stripping Process of a Low Energy Au^- Beam; Dec. 1994

NIFS-326 I. Viniar and S. Sudo,
New Pellet Production and Acceleration Technologies for High Speed Pellet Injection System "HIPEL" in Large Helical Device; Dec. 1994

NIFS-327 Y. Hamada, A. Nishizawa, Y. Kawasumi, K. Kawahata, K. Itoh, A. Ejiri, K. Toi, K. Narihara, K. Sato, T. Seki, H. Iguchi, A. Fujisawa, K. Adachi, S. Hidekuma, S. Hirokura, K. Ida, M. Kojima, J. Koong, R. Kumazawa, H. Kuramoto, R. Liang, T. Minami, H. Sakakita, M. Sasao, K.N. Sato, T. Tsuzuki, J. Xu, I. Yamada, T. Watari,
Fast Potential Change in Sawteeth in JIPP T-IIU Tokamak Plasmas; Dec. 1994

NIFS-328 V.D. Pustovitov,
Effect of Satellite Helical Harmonics on the Stellarator Configuration; Dec. 1994

NIFS-329 K. Itoh, S-I. Itoh and A. Fukuyama,
A Model of Sawtooth Based on the Transport Catastrophe; Dec. 1994

NIFS-330 K. Nagasaki, A. Ejiri,
Launching Conditions for Electron Cyclotron Heating in a Sheared Magnetic Field; Jan. 1995

NIFS-331 T.H. Watanabe, Y. Todo, R. Horiuchi, K. Watanabe, T. Sato,
An Advanced Electrostatic Particle Simulation Algorithm for Implicit Time Integration; Jan. 1995

NIFS-332 N. Bekki and T. Karakisawa,
Bifurcations from Periodic Solution in a Simplified Model of Two-dimensional Magnetoconvection; Jan. 1995

NIFS-333 K. Itoh, S.-I. Itoh, M. Yagi, A. Fukuyama,
Theory of Anomalous Transport in Reverse Field Pinch; Jan. 1995

NIFS-334 K. Nagasaki, A. Isayama and A. Ejiri
Application of Grating Polarizer to 106.4GHz ECH System on Heliotron-E; Jan. 1995

NIFS-335 H. Takamaru, T. Sato, R. Horiuchi, K. Watanabe and Complexity Simulation Group,
A Self-Consistent Open Boundary Model for Particle Simulation in Plasmas; Feb. 1995

NIFS-336 B.B. Kadomtsev,
Quantum Telegragh : is it possible?; Feb. 1995

NIFS-337 B.B.Kadomtsev,
Ball Lightning as Self-Organization Phenomenon; Feb. 1995

NIFS-338 Y. Takeiri, A. Ando, O. Kaneko, Y. Oka, K. Tsumori, R. Akiyama, E. Asano, T. Kawamoto, M. Tanaka and T. Kuroda,
High-Energy Acceleration of an Intense Negative Ion Beam; Feb. 1995

NIFS-339 K. Toi, T. Morisaki, S. Sakakibara, S. Ohdachi, T.Minami, S. Morita, H. Yamada, K. Tanaka, K. Ida, S. Okamura, A. Ejiri, H. Iguchi, K. Nishimura, K. Matsuoka, A. Ando, J. Xu, I. Yamada, K. Narihara, R. Akiyama, H. Idei, S. Kubo, T. Ozaki, C. Takahashi, K. Tsumori,
H-Mode Study in CHS; Feb. 1995

NIFS-340 T. Okada and H. Tazawa,
Filamentation Instability in a Light Ion Beam-plasma System with External Magnetic Field; Feb. 1995

NIFS-341 T. Watanbe, G. Gnudi,
A New Algorithm for Differential-Algebraic Equations Based on HIDM; Feb. 13, 1995

NIFS-342 Y. Nejoh,
New Stationary Solutions of the Nonlinear Drift Wave Equation; Feb. 1995

NIFS-343 A. Ejiri, S. Sakakibara and K. Kawahata,
Signal Based Mixing Analysis for the Magnetohydrodynamic Mode Reconstruction from Homodyne Microwave Reflectometry; Mar.. 1995

NIFS-344 B.B.Kadomtsev, K. Itoh, S.-I. Itoh
Fast Change in Core Transport after L-H Transition; Mar. 1995

NIFS-345 W.X. Wang, M. Okamoto, N. Nakajima and S. Murakami,
An Accurate Nonlinear Monte Carlo Collision Operator; Mar. 1995

NIFS-346 S. Sasaki, S. Takamura, S. Masuzaki, S. Watanabe, T. Kato, K. Kadota,
Helium I Line Intensity Ratios in a Plasma for the Diagnostics of Fusion Edge Plasmas; Mar. 1995

NIFS-347 M. Osakabe,
Measurement of Neutron Energy on D-T Fusion Plasma Experiments; Apr. 1995

NIFS-348 M. Sita Janaki, M.R. Gupta and Brahmananda Dasgupta,
Adiabatic Electron Acceleration in a Cnoidal Wave; Apr. 1995

NIFS-349 J. Xu, K. Ida and J. Fujita,
A Note for Pitch Angle Measurement of Magnetic Field in a Toroidal Plasma Using Motional Stark Effect; Apr. 1995

NIFS-350 J. Uramoto,
Characteristics for Metal Plate Penetration of a Low Energy Negative Muonlike or Pionlike Particle Beam: Apr. 1995

NIFS-351 J. Uramoto,
An Estimation of Life Time for A Low Energy Negative Pionlike Particle Beam: Apr. 1995

NIFS-352 A. Taniike,
Energy Loss Mechanism of a Gold Ion Beam on a Tandem Acceleration System: May 1995

NIFS-353 A. Nishizawa, Y. Hamada, Y. Kawasumi and H. Iguchi,
Increase of Lifetime of Thallium Zeolite Ion Source for Single-Ended Accelerator: May 1995

NIFS-354 S. Murakami, N. Nakajima, S. Okamura and M. Okamoto,
Orbital Aspects of Reachable β Value in NBI Heated Heliotron/Torsatrons; May 1995

NIFS-355 H. Sugama and W. Horton,
Neoclassical and Anomalous Transport in Axisymmetric Toroidal Plasmas with Electrostatic Turbulence; May 1995

NIFS-356 N. Ohyabu
A New Boundary Control Scheme for Simultaneous Achievement of H-mode and Radiative Cooling (SHC Boundary); May 1995

NIFS-357 Y. Hamada, K.N. Sato, H. Sakakita, A. Nishizawa, Y. Kawasumi, R. Liang, K. Kawahata, A. Ejiri, K. Toi, K. Narihara, K. Sato, T. Seki, H. Iguchi, A. Fujisawa, K. Adachi, S. Hidekuma, S. Hirokura, K. Ida, M. Kojima, J. Koong, R. Kumazawa, H. Kuramoto, T. Minami,. M. Sasao, T. Tsuzuki, J.Xu, I. Yamada, and T. Watari,
Large Potential Change Induced by Pellet Injection in JIPP T-IIU Tokamak Plasmas; May 1995

NIFS-358 M. Ida and T. Yabe,
Implicit CIP (Cubic-Interpolated Propagation) Method in One Dimension; May 1995

NIFS-359 A. Kageyama, T. Sato and The Complexity Simulation Group,
Computer Has Solved A Historical Puzzle: Generation of Earth's Dipole Field; June 1995

NIFS-360 K. Itoh, S.-I. Itoh, M. Yagi and A. Fukuyama,
Dynamic Structure in Self-Sustained Turbulence; June 1995

NIFS-361 K. Kamada, H. Kinoshita and H. Takahashi,
Anomalous Heat Evolution of Deuteron Implanted Al on Electron Bombardment; June 1995

NIFS-362 V.D. Pustovitov,
Suppression of Pfirsch-schlüter Current by Vertical Magnetic Field in Stellarators; June 1995

NIFS-363 A. Ida, H. Sanuki and J. Todoroki
An Extended K-dV Equation for Nonlinear Magnetosonic Wave in a Multi-Ion Plasma; June 1995

NIFS-364 H. Sugama and W. Horton
Entropy Production and Onsager Symmetry in Neoclassical Transport Processes of Toroidal Plasmas; July 1995

NIFS-365 K. Itoh, S.-I. Itoh, A. Fukuyama and M. Yagi,
On the Minimum Circulating Power of Steady State Tokamaks; July 1995

NIFS-366 K. Itoh and Sanae-I. Itoh,
The Role of Electric Field in Confinement; July 1995

NIFS-367 F. Xiao and T. Yabe,
A Rational Function Based Scheme for Solving Advection Equation; July 1995

NIFS-368 Y. Takeiri, O. Kaneko, Y. Oka, K. Tsumori, E. Asano, R. Akiyama, T. Kawamoto and T. Kuroda,
Multi-Beamlet Focusing of Intense Negative Ion Beams by Aperture Displacement Technique; Aug. 1995

NIFS-369 A. Ando, Y. Takeiri, O. Kaneko, Y. Oka, K. Tsumori, E. Asano, T. Kawamoto, R. Akiyama and T. Kuroda,
Experiments of an Intense H- Ion Beam Acceleration; Aug. 1995

NIFS-370 M. Sasao, A. Taniike, I. Nomura, M. Wada, H. Yamaoka and M. Sato,
Development of Diagnostic Beams for Alpha Particle Measurement on ITER; Aug. 1995

NIFS-371 S. Yamaguchi, J. Yamamoto and O. Motojima;
A New Cable -in conduit Conductor Magnet with Insulated Strands; Sep. 1995

NIFS-372 H. Miura,
Enstrophy Generation in a Shock-Dominated Turbulence; Sep. 1995